

TIME RESOLVED LIDAR FLUOROSENSOR  
OPERATING FROM HELICOPTER

Alfredo Bianchi, Alberto Gallotti

Agusta S.p.A. - U. d. B. Sistemi e Spazio  
Tradate (Varese) - Italy

Claudio Koechler, Jean Verdebout

Commission of European Communities  
Joint Research Center (JRC)  
Ispra (Varese) - Italy

Abstract

Lidar (Light Detection and Ranging) techniques are earning more and more interest in remote sensing applied to pollution detection and monitoring of water and air, allowing the characterization of the pollutant factors by qualitative and quantitative analysis.

The possibility to perform environmental surveys from helicopters, that are platforms able to operate in critical conditions and with a reduced logistic support, allowing both measurements on quite large areas and measurements on precise points by hovering, makes this kind of sensors more and more interesting as scientific tools to be used in support of legal or political actions.

Agusta is making a Time Resolved Lidar Fluorosensor (TRLF) compatible with the helicopter.

This TRLF, unique in the world in its conceptual configuration, has been jointly designed and realized by JRC-Ispra and CISE-Milano; Agusta is performing validation tests in order to assess the applications operating it from an AB 412 and verifying the helicopter compatibility.

This sensor is particularly suitable for oil characterization (identification) and in the analysis of water column parameters.

1. Introduction

1.1 Principle of operation

The Lidar technique is applied to a variety of environmental investigations.

Its importance lies in the peculiar sensitivity and

spectrochemical coverage of the fluorescent emission, which makes this technique a comprehensive tool for the analysis of remote targets.

The Time Resolved Lidar Fluorosensor (TRLF) has been designed for the characterization of oil slicks and for the investigation of water column parameters.

The instrument implements an active technique in which the target signal is induced by a short (1 nsec.) laser pulse. If the pulse hits an oil slick or organic matter, it induces a fluorescence; a part of this light is collected by the system telescope and processed.

The spectro-temporal analysis of the return signal allows the characterization.

#### 1.1.1 Identification (fingerprinting) of crude oils

The various oils transported in the Mediterranean sea, largely differ in their laser induced fluorescence intensity (yield) but the spectral distribution of the emitted light (with excitation at 355 nm) always takes slope of a broad, almost featureless peak, covering the visible region, having maximum between 420 nm and 480 nm (Fig.1).

The fluorescence yield information is difficult to recover with a remote sensing technique, as it implies a very accurate and stable sensitivity calibration. In this way, it is difficult to define a fingerprinting procedure.

Extended laboratory studies showed that for the same oil, the decay time depends on the analysed wavelength, being shorter at shorter wavelength.

It have been also showed that the decay times are strongly dependent on the type of oil (Fig.2 and Fig.3).

Having both spectral and temporal resolution, the TRLF meets the requirements for oil identification.

#### 1.1.2 Probing the water column

Due to its temporal resolution, the sensor can also be used for water column analysis, giving information on water optical properties, quantity of suspended and dissolved organic matter and phytoplankton concentration.

In fact, a laser pulse penetrating into the water, is subject to the following interactions:

- elastic scattering due to water molecules (Rayleigh) and suspended matter (Mie);
- inelastic diffusion by water molecules (Raman);
- absorption with induced fluorescence of organic matter (Gelbstoff) and phytoplankton.

Analysing the backscattered light and the Raman diffusion, it is possible to measure the extinction coefficient of the water, that is an important indicator of the water quality. The Raman signal provides a way to normalize the other signals and to evaluate the concentration of dissolved organic carbon (DOC), suspended matter and Phytoplankton.

The water column response is also important for the validation of the measurements on oils.

The Gelbstoff fluorescence is similar to that of the oils and there is the possibility to mistake a Gelbstoff signal for a weak signal produced by a thin film.

The TRLF provides a clue to distinguish these responses: the Gelbstoff signal shows a build-up time due to its distribution in the water, while the oil-film signal rises as steeply as the exciting laser pulse.

In Fig.4 and 5 spectra and spectro-temporal images of clear water and with added organic acid are shown.

In Fig.6 are shown time decays of backscattering, Raman diffusion and DOM fluorescence signals.

## 2. Design of the Time Resolved Lidar Fluorosensor

### 2.1 Conceptual Design

The exciting source is an actively mode locked Nd:YAG laser with second and third harmonic generation.

For normal operations, the third harmonic (355 nm) is used. At this wavelength, the pulse duration is 1 nsec. and the maximum output energy is 30 mJ.

The second harmonic (532 nm) is particularly interesting for water column analysis; at this wavelength, the energy is 60 mJ.

The beam diameter at the telescope output is about 3 cm, with a divergence of 0.15 mrad.

The operating firing rate of the laser can range from 1 p.p.s. up to 10 p.p.s.

The output beam is actively maintained aligned on the telescope axis by a feedback mechanism acting on one of the output mirrors.

The receiving telescope is a Newtonian one with a diameter of 30 cm and a focal length of 85 cm.

At the focal point, the light is collected by an optical fiber which brings the signal to the spectro-temporal analyser.

The position of the fiber input is automatically adjusted as a function of the target distance, in order to optimize the collection efficiency.

A polychromator provides the spectral dispersion of the collected signal and a streak-camera realizes the temporal dispersion in the direction perpendicular to the spectral one.

The spectro-temporal image is created on a phosphor screen, is intensified by a Micro Channel Plate (MCP) and read by a CCD detector.

Two spectral ranges are available: 360 nm or 260 nm wide.

Both can be centered as requested by the measurement.

The available temporal windows are 30 nsec and 75 nsec with corresponding resolution of 1 nsec and 2.5 nsec.

The streak-camera needs to receive a triggering signal with an advance of about 40 nsec with respect to the incoming light signal.

Since the trigger must be generated by the returned signal, a fraction of this is diverted to a photomultiplier for providing the trigger itself, while the remaining part is delayed by the optical fiber connecting the telescope with the streak-camera.

The CCD camera image is processed, for each laser shot, by a read-out system and the digital data are transmitted to a VAX station GPX II and stored onto a Hard disk.

The analysis of the data has to be performed off line, but the measured signals are displayed in real time to the operator.

The VAX microcomputer display includes information such as laser pulse energy, target distance, streak-camera gain, etc.

A conceptual layout of the TRLF is shown in Fig.7.

The system is splitted in six subsystems; five of them, including electronics, are packaged into avionic boxes.

The sixth is the folding mirror, the function of this is to deflect the laser beam to the water surface and to collect the return signal sending it to the telescope.

## 2.2 Technical specifications

### 2.2.1 Optical subsystem

- Laser type	Nd:YAG, mode locked, SFUR
- Wavelength	532 nm (green); 355 nm (UV)
- Energy	60 mJ; 30 mJ
- Pulse duration	1 nsec.
- Pulse repetition rate	up to 10 pulse per second
- Beam divergence	0.15 mrad (after beam exp.)
- Pointing stability	0.15 mrad
- Telescope aperture	30 cm
- Telescope focal length	85 cm
- Receiver spectral range	350-710 nm
- Spectral resolution	15 nm
- Receiver optical efficiency	15 %
- Receiver FOV	0.35 mrad

2.2.2 Detection and Data Acquisition Subsystem

- Temporal ranges 30 nsec; 75 nsec
- Temporal resolution 1 nsec; 2.5 nsec
- Data acquisition system MicroVAX GPX II
- Mass memory 70 Mbytes
- Real time data display fluorescence, Raman, laser signals

2.2.3 Operational features

- Number of operators 1 or 2
- Working temperature 5°C to 30°C
- Helicopter operating altitude 300 ft to 800 ft

2.2.4 Mechanical and Electrical Characteristics

The system actual dimension for each part and the respective power consumption (when the laser is operated at 10 p.p.s.) are showed in Tab.1.

	Dimensions (mm)			Weight kg	DC 28 V	110 V 400 Hz
	W	H	D			
A	550	620	820	79	800 W	
B	550	530	690	44		500 W
C	1200	900	860	243	450 W	50 W
D						
E	550	620	690	80	50 W	650 W
F	550	620	690	53	300 W	
Total				499	1600 W	1200 W

- A VAX station GPX II, videorecorder, TV screen and streak camera monitor
- B streak camera electronics
- C laser head, transmission and collecting optics, telescope, streak camera, electronics
- D output mirror
- E laser power supply and controls
- F VAX station terminal.

Tab.1 - TRLF mechanical and electrical characteristics.

3. TRLF installation on Agusta AB 412 Helicopter

3.1 Mechanical installation

The actual system was originally designed for fixed-wing aircraft installation. Fortunately, no mechanical change has been required, due to the cabin volume of the AB 412 helicopter.

Even if a great part of the helicopter cabin is occupied by the system, sufficient area for two operators is available, in order to permit good operability. The installation layout is shown in Fig.8.

### 3.2 Electrical installation

The high power consumption has required a significant change in the operation.

In the basic version of AB 412, the alternate current is not generated by an alternator but is derived by inverters from the 28 Vdc and no alternator can supply more than 450 VA, so a supplementary inverter of 600 VA has been installed into the cabin.

At the same time, the laser is operated with a shot rate of 2 Hz, in order to reduce the consumption of the laser power supply down to 100 W at 110 Vac.

The streak-camera read out subsystem is powered by the supplementary inverter.

### 3.3 TRLF compatibility with AB 412 helicopter

#### 3.3.1 Mechanical compatibility

The pressure on the floor is within the specs for the AB 412.

Due to the fact that all the subsystems are already packaged into avionics boxes, preliminary tests on the helicopter were directly performed.

For reducing effects of vibrations at low frequencies, large strips of rubber were put under all the boxes set on the floor of the cabin.

Vibrational tests were done in the following way:

a. On ground, with the helicopter blades rotating, the system powered an the laser firing to a target at a distance of 150 meters.

The beam was stable in pointing direction within 2 mrad. No damage occurred at the system due to the helicopter vibrations.

b. Flying, with the system completely powered and the laser beam stopped at the exit of the telescope.

No damage occurred due to the helicopter vibrations.

#### 3.3.2 Electromagnetic compatibility (EMC)

No EM interference between helicopter avionics/transmission systems and the TRLF partially and completely powered and operated was verified during the above test b.

### 3.4 Preliminary system improvements

Only few little mechanical modification have been introduced in order to improve the safety of some critical part in the detection module.

Some rubber and foam have been introduced in order to reduce the possibility of movements between optical parts in mechanical contact (CCD/MCP).

Siliconic gum has been put on some electronic component of the streak-camera.

No electrical modification has been performed.

Two ON/OFF switches have been added for turning off the laser in emergency, one for the Pilot, the other for the second operator, giving the possibility to avoid to send the laser beam when needed.

### 3.5 Flight test of the instrument

The LIDAR has been tested during two flights performed over the sea. The instrument was operated with a firing rate of 2 Hz, acquiring the spectro-temporal signal at each shot. In these conditions, for reasons of data throughput, the full resolution of the CCD (576x385) cannot be maintained and it is necessary to read the CCD by micropixels in which the charges contained in blocks of 30 pixels (5x6) are summed. The operating altitude was 300 feet and the third harmonic was used as the excitation wavelength.

Figure 9 shows a typical time-integrated spectrum of a single shot measurement: the backscattering and Raman diffusion peaks are superimposed on the spectrally broad fluorescence of the dissolved organic matter (DOM). As expected, this last signal is much smaller for sea water than for the lake water used in the laboratory simulation experiments (see figure 4).

Figure 10 shows the time dependence of the backscattering and Raman signals, extracted from the same measurement. Both the signals show an exponential decay from which it is possible to determine the water extinction coefficient ( $k$ ) at the correspondent wavelength (355 and 404 nm).

Figure 11 shows the time dependence of the fluorescence signals: the top curve corresponds to the normal DOM signal; in the case of the measurement represented by the lower curve, a thin (semi-transparent) film of oil was present on the sea. The oil fluorescence is distinguishable because, as it came from the surface, it is detected before the DOM fluorescence. Nevertheless, the two signals are partly mixed and the fingerprinting procedure is not readily applicable in such a limiting case.

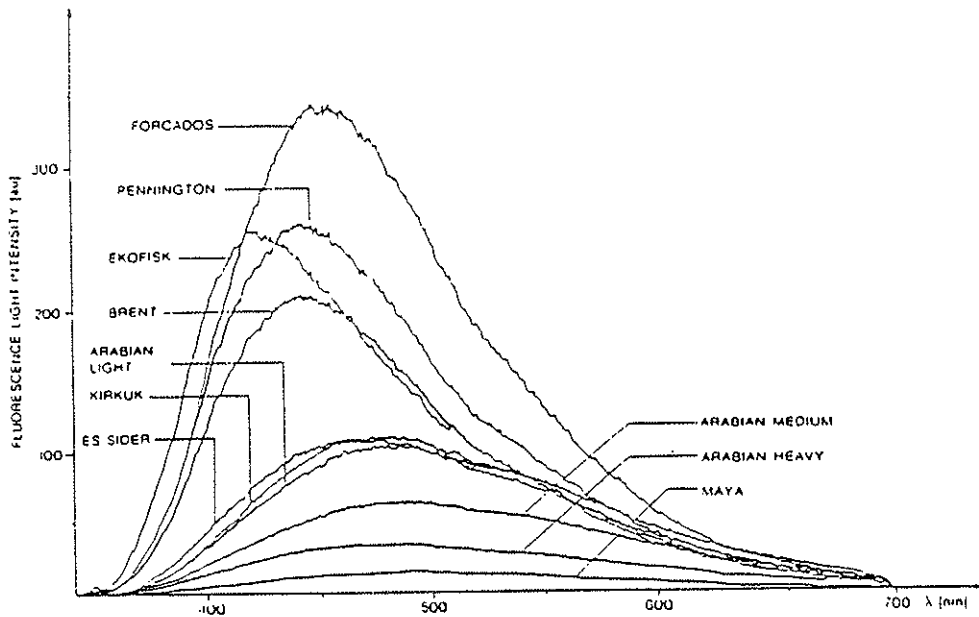


Fig. 1 - Fluorescence spectra of various crude oils.

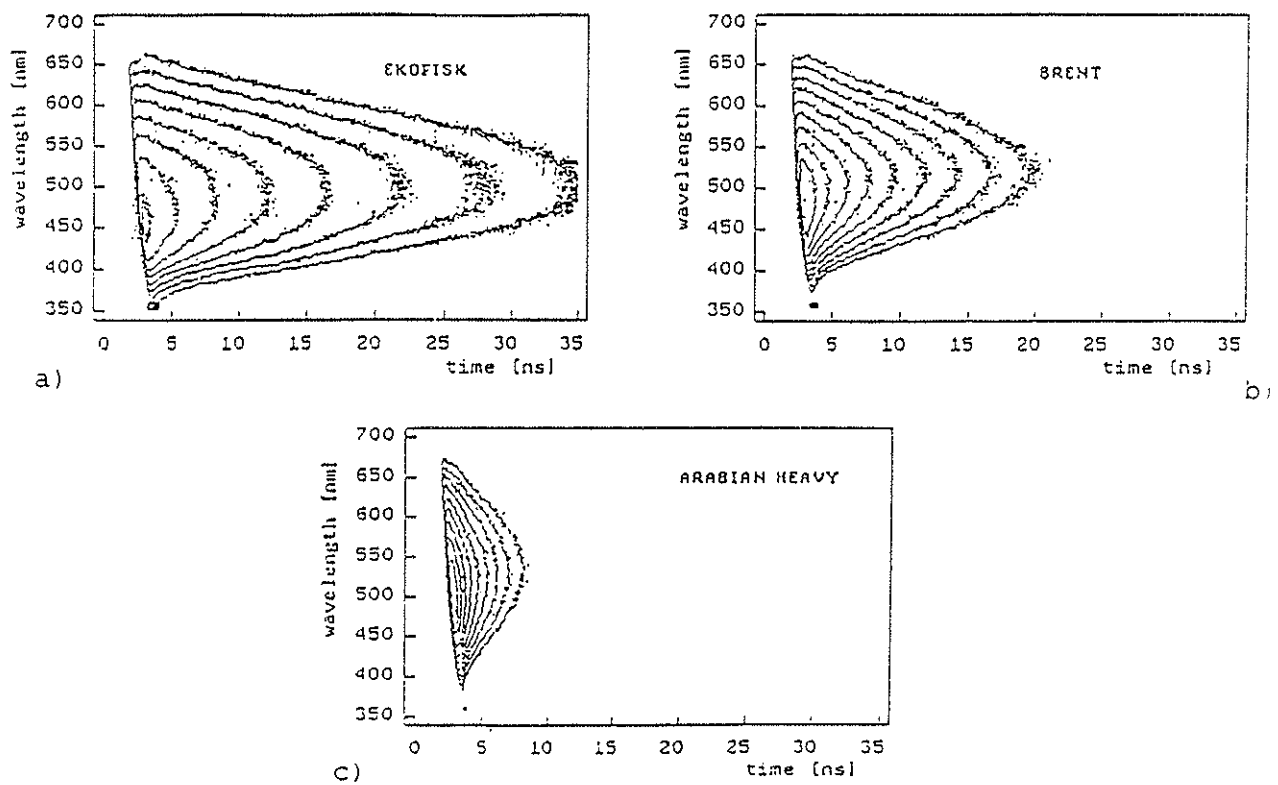


Fig. 2 - Time resolved spectra: a) light crude oil, b) medium crude oil, c) heavy crude oil.



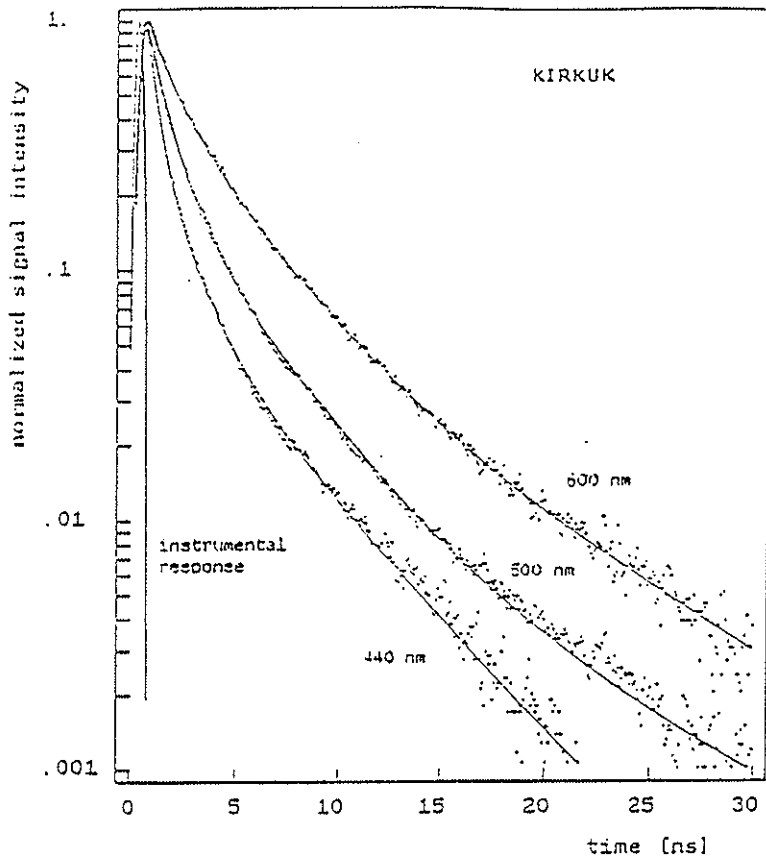


Fig. 3 - Time decay for Kirkuk oil emission at 440 nm, 500 nm & 600 nm wavelength.

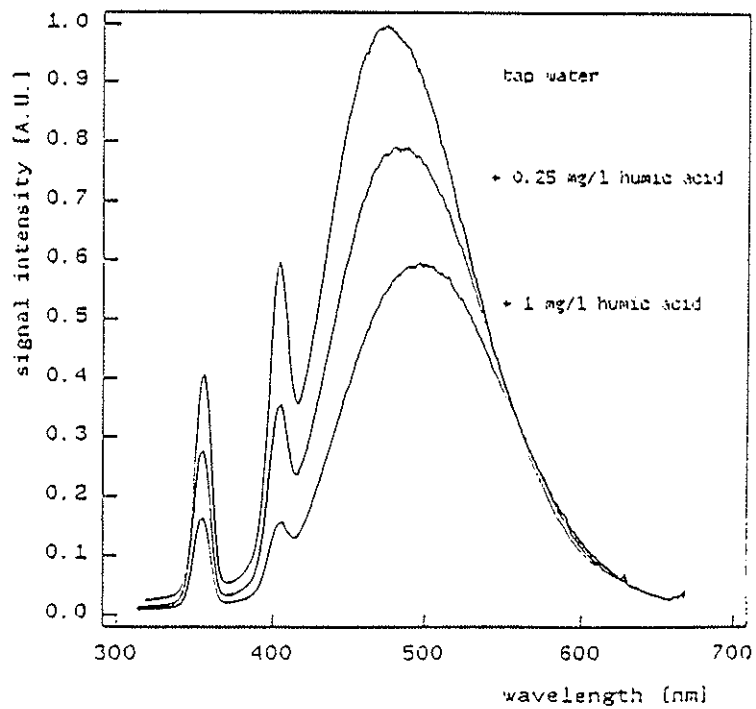


Fig. 4- Spectra of clear water and water with organic acid added.

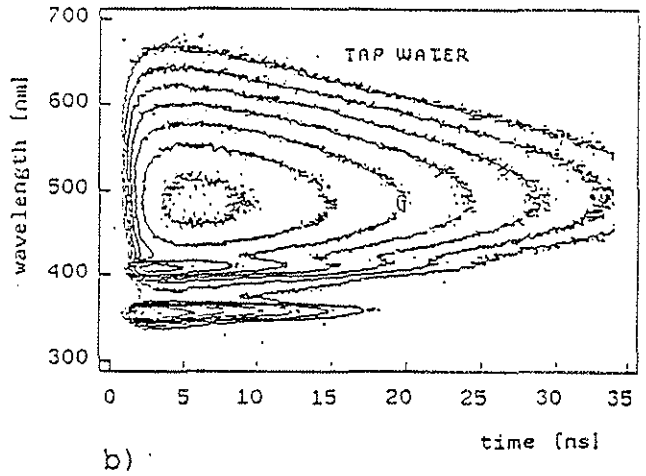
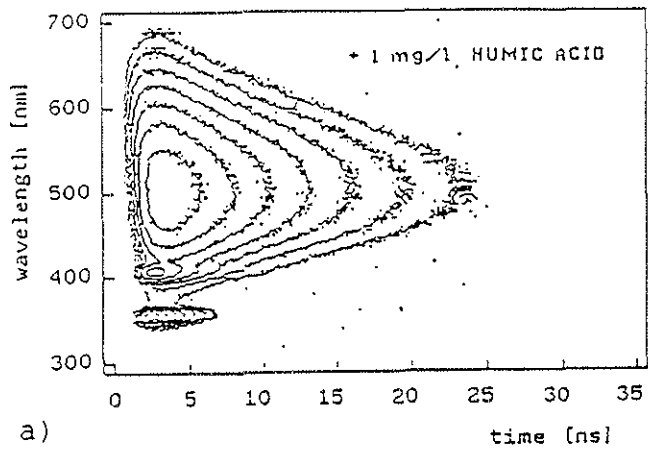


Fig. 5- Spectro-temporal image of water:  
 a) with organic acid  
 b) clear water.

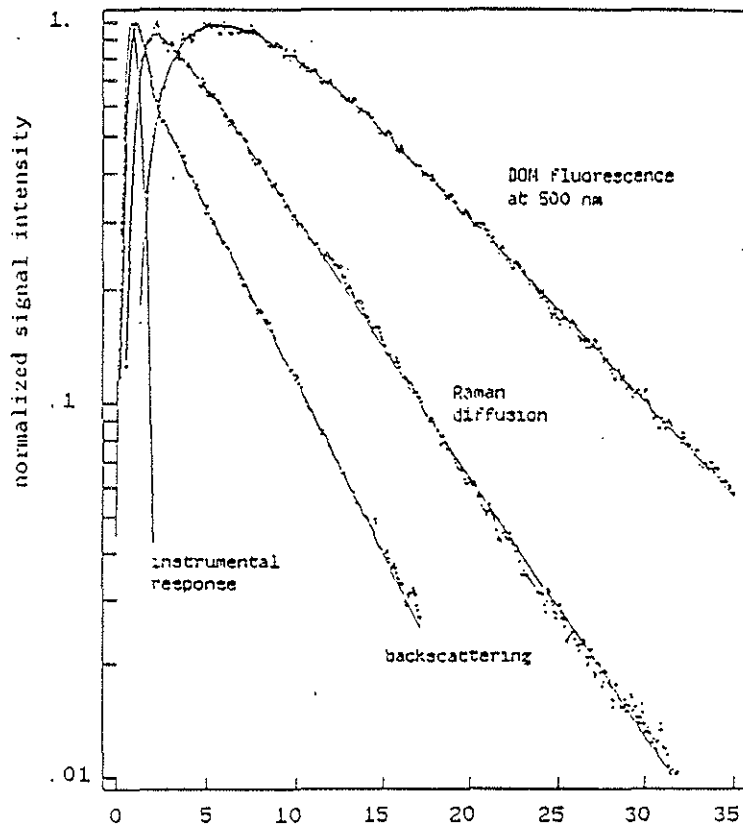


Fig. 6- Time decays for backscattered signal, Raman diffusion and DOM fluorescence

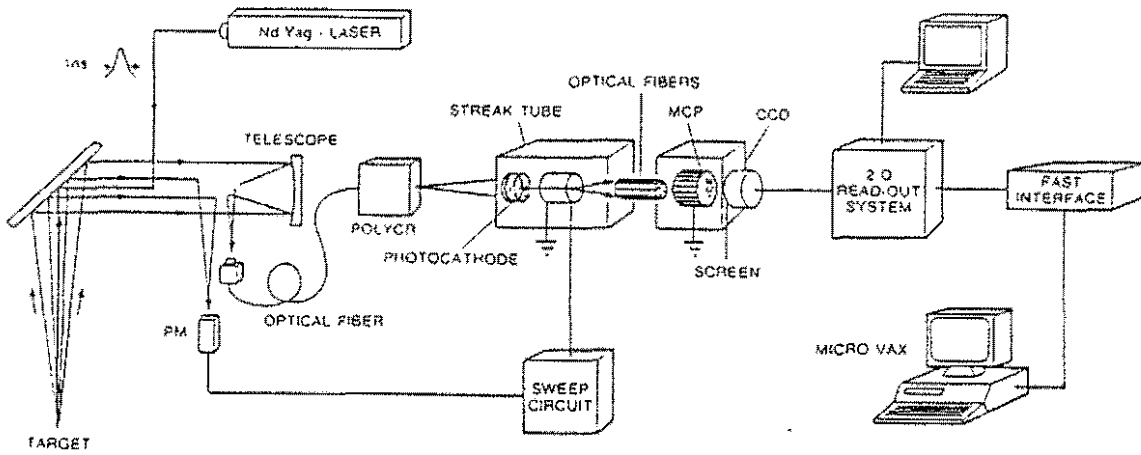


Fig. 7- Conceptual lay-out of TRLF

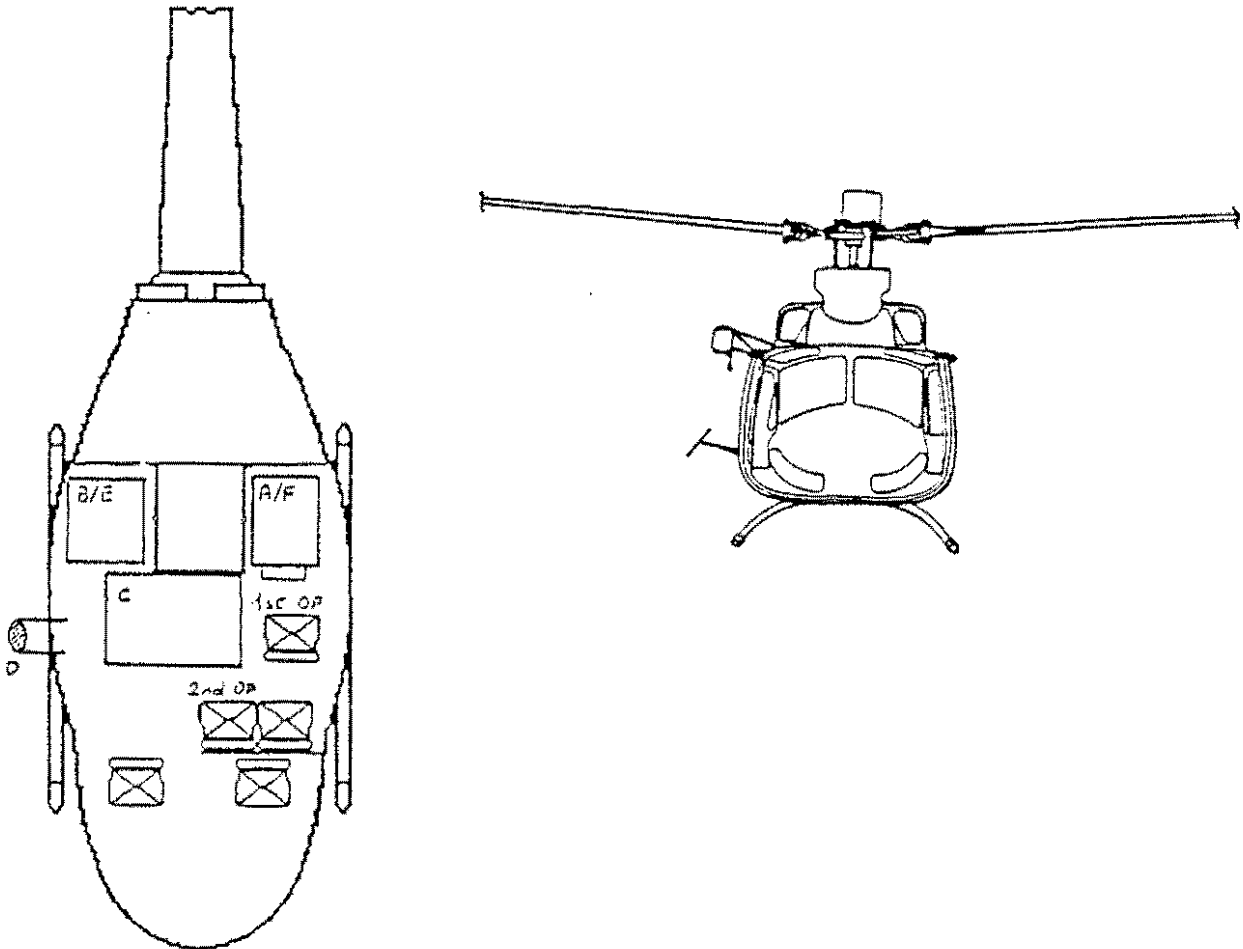


Fig. 8- TRLF installation on the AB 412 helicopter

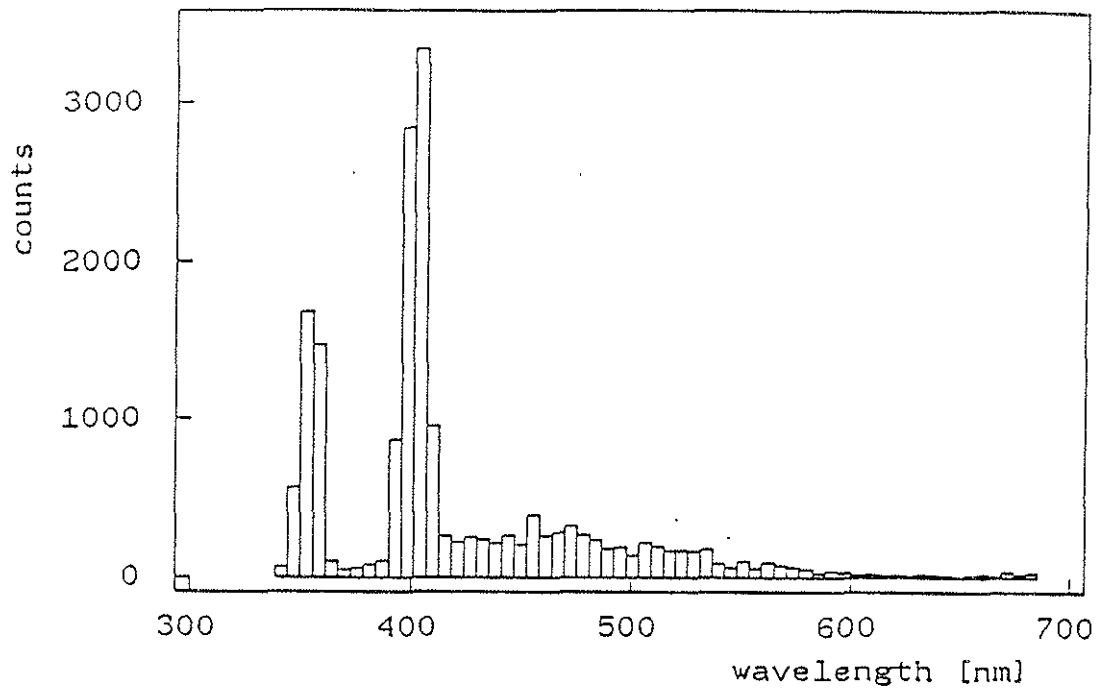


Fig. 9 - Time integrated spectrum of a single shot measurement on sea water, performed from the helicopter operating at 300 ft.

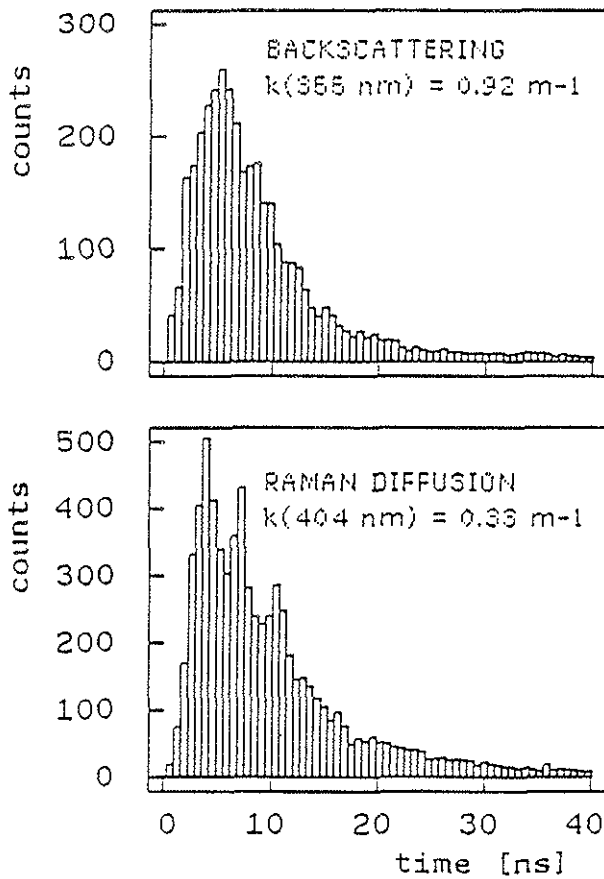


Fig. 10 - Time dependence of the backscattering and Raman signals.

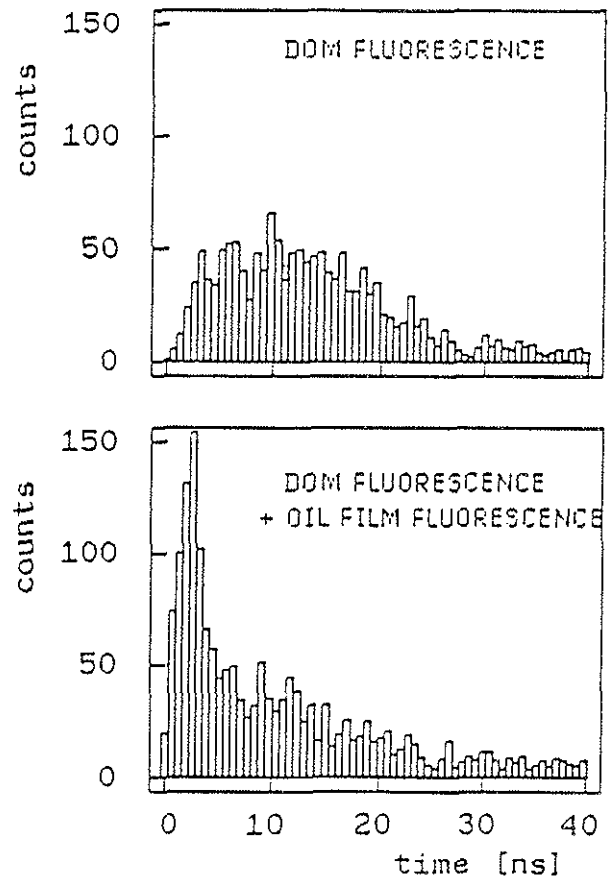


Fig. 11 - Time dependence of fluorescence signals.